Performance Optimizing Multi-Objective Adaptive Control with Time-Varying Model Reference Modification

Nhan T. Nguyen[a]
NASA Ames Research Center, Moffett Field, CA 94035
Kelley E. Hashemi[b]
Universities Space Research Association, Moffett Field, CA 94035
Tansel Yucelen[c]
University of South Florida, FL 33620
Ehsan Arabi[d]
University of South Florida, FL 33620

This paper presents a new adaptive control approach that involves a performance optimization objective. The problem is cast as a multi-objective optimal control. The control synthesis involves the design of a performance optimizing controller from a subset of control inputs. The effect of the performance optimizing controller is to introduce an uncertainty into the system that can degrade tracking of the reference model. An adaptive controller from the remaining control inputs is designed to reduce the effect of the uncertainty while maintaining a notion of performance optimization in the adaptive control system.

I. Introduction

Model-reference adaptive control (MRAC) has been developed with the prime purpose of reducing the tracking error between a plant and a reference model. In this context, it is viewed as a nonlinear integral feedback control with a learning algorithm. There is a wealth of knowledge in MRAC with various modifications and extensions. In many aerospace applications, oftentimes there may be multiple control requirements imposed on a flight control system. For example, for flexible aircraft flight control, tracking of a flight control command is usually performed by a flight control system while the response of elastic modes is suppressed passively by a notch filter. If there is a redundancy in flight control actuation in a flight vehicle, such a flight control task may be feasible.

The modal suppression in the example could be performed actively by additional control actuators.[1] In this work, we develop a multi-objective performance-based adaptive optimal control with the goal of providing adaptation while seeking to minimize a performance metric. This performance metric could be any signal from the plant that needs to be minimized such as aerodynamic drag force on an aircraft or gust load response of a flexible wing structure. Multi-objective adaptive control has been developed by Nguyen[2–4] in the recent years. Bi-objective optimal control modification extends the optimal control modification adaptive law to improve tracking performance of systems with input uncertainty and matched uncertainty. The adaptive law seeks to minimize both the tracking error and the predictor error which are used in the adaptation. A further extension of this work led to the development of multi-objective optimal control modification which seeks to minimize the effect of unmatched uncertainty.[3] In the context of aircraft flight control, multi-objective optimal control has been developed to address specifically drag minimization, flutter suppression, and maneuver load alleviation for flexible aircraft. This method results in a modified Ricatti equation which takes into account the drag and maneuver load sensitivities which are assumed to be known.[5–7] By leveraging this approach, the present study extends this work by addressing unknown performance sensitivities which require a least-squares parameter estimation coupled with a time-varying modified Ricatti equation.

[a]Technical Group Lead and Senior Research Scientist, Intelligent Systems Division, AIAA Associate Fellow, nhan.t.nguyen@nasa.gov
[b]NASA Post-Doctoral Fellow, Intelligent Systems Division, kelley.e.hashemi@nasa.gov
[c]Assistant Professor and Director of the Laboratory for Autonomy, Control, Information, and Systems, yucelen@lacis.team
[d]Graduate Research Assistant, ehsanarabi@mail.usf.edu

This study differs in those previous concepts in that a performance metric is optimized by an optimal control action provided by a subset of control inputs while the adaptation to suppress the effect of matched uncertainty is provided by another subset of the control inputs. The effect of the performance optimizing control is to modify the original reference model in order to meet the performance objective. This reference model modification is accomplished by adding time-varying gain matrices to the original linear time-invariant reference model. The time-varying gain matrices are computed by a real-time Ricatti equation coupled with parameter estimation of the performance metric. The adaptive control is then designed to track the time-varying modified reference model.

There exists a trade-off between tracking and performance optimization. The adaptive control can reduce the effect of the performance optimizing control to a sufficient degree to maintain reasonable tracking performance without eliminating the benefit of the performance optimizing control. This approach could bring promise to adaptive control by enabling optimal control to co-exist in a MRAC design for performance optimizing adaptation.

The performance optimizing adaptive control is demonstrated in simulations of a maneuver load alleviation control of a flexible wing Generic Transport Model (GTM) during a pull-up maneuver. The simulations demonstrate the effectiveness of the performance optimizing adaptive control.

II. Performance Optimizing Adaptive Control

Consider a plant model

$$\dot{x} = Ax + B\left[u + \Theta^{*\top}\Phi(x)\right] \tag{1}$$

where $x(t) \in \mathbb{R}^n$ is the state vector, $u(t) \in \mathbb{R}^m$ is the control vector, $\Theta^* \in \mathbb{R}^{l\times m}$ is an unknown constant matrix that represents a matched uncertainty, $\Phi(x) \in \mathbb{R}^l$ is a known function, and $A \in \mathbb{R}^{n\times n}$ and $B \in \mathbb{R}^{n\times m}$ are known matrices. The plant is considered to be a full-state system with all the available states for control.

The plant is associated with a performance metric

$$y = Cx + Du \tag{2}$$

where $y(t) \in \mathbb{R}$ is a performance metric for the plant, and $C \in \mathbb{R}^n$ and $D \in \mathbb{R}^m$ are matrices which can be known or unknown. The nature of the performance metric is dependent on the plant model. In some cases, $y(t)$ is available from a measurement, but the matrices C and D are unknown. Then, the matrices C and D have to be estimated. In other cases, $y(t)$ is not measured, but the matrices C and D are known precisely so that $y(t)$ can be computed.

The goal is to design an adaptive controller that enables the plant to track a reference model

$$\dot{x}_m = A_m x_m + B_m r \tag{3}$$

while minimizing the performance metric of the plant.

Thus, the adaptive controller has to satisfy simultaneously two objectives: tracking the reference model and minimization of the performance metric. We assume there exists a sufficient number of control inputs that can satisfy both objectives simultaneously. Let $u(t) = \begin{bmatrix} u_a^\top(t) & u_p^\top(t) \end{bmatrix}^\top$ where $u_a(t) \in \mathbb{R}^p$ is a control vector dedicated to suppressing the matched uncertainty and $u_p(t) \in \mathbb{R}^{m-p}$ is a control vector dedicated to optimizing the plant's performance. Correspondingly, let $B = \begin{bmatrix} B_a & B_p \end{bmatrix}$ be the control sensitivity matrix comprising an adaptive component $B_a \in \mathbb{R}^{n\times p}$ and a performance optimization component $B_p \in \mathbb{R}^{n\times m-p}$. Similarly, we decompose the matched uncertainty into the corresponding components $\Theta_a^* \in \mathbb{R}^{l\times p}$ and $\Theta_p^* \in \mathbb{R}^{l\times m-p}$.

Then, we write

$$\dot{x} = Ax + B_a u_a + B_p u_p + B_a \Theta_a^{*\top}\Phi(x) + B_p \Theta_p^{*\top}\Phi(x) \tag{4}$$

It is obvious that the choice of $u_a(t)$ and $u_p(t)$ can influence the performance of the overall system. The adaptive controller $u_a(t)$ should be chosen such that it can cancel out most of the effect of the matched uncertainty. In some cases, the plant uncertainty may exist in such a way that it could be completely cancelled out. In such cases, $\Theta_p^* = 0$. For simplicity, we will consider this case in this study. Further, we will assume that $u_p(t)$ can only influence the performance metric $y(t)$ such that

$$y = Cx + D_p u_p \tag{5}$$

We design an adaptive controller as follows:

$$u_a = K_x x + K_r r - u_{ad} \tag{6}$$

where $A+B_aK_x \in \mathbb{R}^{n\times n}$ is Hurwitz and $r(t) \in \mathbb{R}^q$ is a bounded reference command signal.

The reference model is chosen to be the closed-loop nominal plant so that $A_m = A+B_aK_x$ and $B_m = B_aK_r$.

Then, the plant becomes

$$\dot{x} = A_m x + B_m r + B_p u_p - B_a u_{ad} + B_a \Theta_a^{*\top} \Phi(x) \tag{7}$$

Since $u_p(t)$ is dedicated to optimizing the performance metric, it will generate an additional control signal that can cause the plant to not follow the reference model precisely. Therefore, the adaptive controller $u_{ad}(t)$ has to cancel out the possible unmatched uncertainty generated by the performance optimizing controller $u_p(t)$.

We consider the case when $y(t)$ is measured but the matrices C and D are unknown. Let $\hat{y}(t)$ be an estimate of $y(t)$ where

$$\hat{y} = \hat{C}x + \hat{D}_p u_p \tag{8}$$

Then, the performance estimation error is computed as

$$e_y = \hat{y} - y = \tilde{C}x + \tilde{D}_p u_p \tag{9}$$

where $\tilde{C}(t) = \hat{C}(t) - C$ and $\tilde{D}_p(t) = \hat{D}_p(t) - D_p$ are the estimation errors of C and D_p, respectively.

To design a performance optimizing control, we consider the nominal plant without the control action by $u_a(t)$. Then, the nominal plant is expressed as

$$\dot{x} = A_m x + B_m r + B_p u_p \tag{10}$$

We now cast this problem in a multi-objective optimization framework by using the following infinite-time-horizon cost function[7]

$$J = \lim_{t_f\to\infty} \frac{1}{2} \int_0^{t_f} \left(e_y^2 + \hat{y}^\top q \hat{y} + u_p^\top R u_p \right) dt \tag{11}$$

where $q > 0$ and $R > 0$.

We formulate an optimal control problem by establishing the following Hamiltonian function

$$H = \frac{1}{2} e_y^2 + \frac{1}{2} q \hat{y} + \frac{1}{2} u_p^\top R u_p + \mu^\top (A_m x + B_m r + B_p u_p) \tag{12}$$

where $\mu(t) \in \mathbb{R}^n$ is an adjoint vector.

Then the necessary conditions of optimality are obtained as

$$\dot{\mu} = -\frac{\partial H}{\partial x}^\top = -q\hat{C}^\top \left(\hat{C}x + \hat{D}_p u_p \right) - A_m^\top \mu \tag{13}$$

$$\frac{\partial H}{\partial u_p}^\top = q\hat{D}_p^\top \left(\hat{C}x + \hat{D}_p u_p \right) + R u_p + B_p^\top \mu = 0 \tag{14}$$

$$\frac{\partial H}{\partial \tilde{C}} = x e_y^\top \tag{15}$$

$$\frac{\partial H}{\partial \tilde{D}_p} = u_p e_y^\top \tag{16}$$

From Eqs. (15) and (16), we obtain the following adaptive laws:

$$\dot{\hat{C}}^\top = -\Gamma_C \frac{\partial H}{\partial \tilde{C}} = -\Gamma_C x e_y^\top \tag{17}$$

$$\dot{\hat{D}}_p^\top = -\Gamma_{D_p} \frac{\partial H}{\partial \tilde{D}_p} = -\Gamma_{D_p} u_p e_y^\top \tag{18}$$

The optimal control $u_p(t)$ is obtained as

$$u_p = -\left(R + q\hat{D}_p^\top \hat{D}_p \right)^{-1} \left(B_p^\top \mu + q\hat{D}_p^\top \hat{C}x \right) \tag{19}$$

We proceed with the assumed solution of $\mu(t)$ having the form[7]

$$\mu = Wx + V \tag{20}$$

subject to the transversality condition $W(t_f) = 0$ and $V(t_f) = 0$.

Upon substitution, we obtain

$$\begin{aligned}\dot{\mu} = \dot{W}x + \dot{V} + W\left\{A_m x + B_m r - B_p\left(R + q\hat{D}_p^\top \hat{D}_p\right)^{-1}\left[B_p^\top (Wx+V) + q\hat{D}_p^\top \hat{C}x\right]\right\} \\ = -q\hat{C}^\top\left\{\hat{C}x - \hat{D}_p\left(R + q\hat{D}_p^\top \hat{D}_p\right)^{-1}\left[B_p^\top (Wx+V) + q\hat{D}_p^\top \hat{C}x\right]\right\} - A_m^\top (Wx+V)\end{aligned} \tag{21}$$

For infinite-time-horizon optimal control, $W(t)$ and $V(t)$ have constant solutions. Thus, $\dot{W}(t) = 0$ and $\dot{V}(t) = 0$. Then, we obtain the following equations:

$$W\bar{A} + \bar{A}^\top W - WB_p\bar{R}^{-1}B_p^\top W + \bar{Q} = 0 \tag{22}$$

$$V = -\left(\bar{A}^\top - WB_p\bar{R}^{-1}B_p^\top\right)^{-1} WB_m r \tag{23}$$

where

$$\bar{A} = A_m - qB_p\bar{R}^{-1}\hat{D}_p^\top \hat{C} \tag{24}$$

$$\bar{Q} = q\hat{C}^\top\left(1 - q\hat{D}_p\bar{R}^{-1}\hat{D}_p^\top\right)\hat{C} \tag{25}$$

$$\bar{R} = R + q\hat{D}_p^\top \hat{D}_p \tag{26}$$

q is chosen such that $\bar{Q} > 0$ which implies

$$q\hat{D}_p\bar{R}^{-1}\hat{D}_p^\top < 1 \tag{27}$$

Equation (22) is the algebraic time-varying Ricatti equation to be solved on-line as the estimates $\hat{C}(t)$ and $\hat{D}(t)$ are updated at each time step. Then, the performance optimizing controller u_p is obtained as

$$u_p = \bar{K}_x(t)x + \bar{K}_r(t)r \tag{28}$$

where

$$\bar{K}_x = -\bar{R}^{-1}\left(B_p^\top W + \hat{D}_p^\top q\hat{C}\right) \tag{29}$$

$$\bar{K}_r = \bar{R}^{-1}B_p^\top\left(\bar{A}^\top - WB_p\bar{R}^{-1}B_p^\top\right)^{-1} WB_m \tag{30}$$

If $x(t)$ and $u_p(t)$ are persistently exciting signals which imply that the reference command signal is PE, then an exponential parameter convergence is achieved. It follows that the estimates $\hat{C}(t)$ and $\hat{D}(t)$ converge to the true values C and D, respectively.[8] Then, $\bar{K}_x(t) \to \bar{K}_x^*$ and $\bar{K}_r(t) \to \bar{K}_r^*$ where

$$\bar{K}_p^* = -\bar{R}^{*-1}\left(B_p^\top W^* + D_p^\top qC\right) \tag{31}$$

$$\bar{K}_r^* = \bar{R}^{*-1}\left(\bar{A}^{*\top} - W^*B_p\bar{R}^{*-1}B_p^\top\right)^{-1} W^*B_m \tag{32}$$

W^* is the solution of the following algebraic Ricatti equation:

$$W^*\bar{A}^* + \bar{A}^{*\top}W^* - W^*B_p\bar{R}^{*-1}B_p^\top W^* + \bar{Q}^* = 0 \tag{33}$$

where

$$\bar{A}^* = A_m - B_p\bar{R}^{*-1}D_p^\top qC \tag{34}$$

$$\bar{Q}^* = C^\top qC - C^\top qD_p\bar{R}^{*-1}D_p^\top qC \tag{35}$$

$$\bar{R}^* = R + D_p^\top q D_p \tag{36}$$

The proof for parameter convergence is as follows:

Proof: Choose a Lyapunov candidate function

$$V\left(\tilde{C},\tilde{D}\right) = \tilde{C}\Gamma_C^{-1}\tilde{C}^\top + \tilde{D}_p\Gamma_{D_p}^{-1}\tilde{D}_p^\top \tag{37}$$

Then, $\dot{V}\left(\tilde{C},\tilde{D}\right)$ is evaluated as

$$\dot{V}\left(\tilde{C},\tilde{D}\right) = -2\tilde{C}xe_y^\top - 2\tilde{D}_p u_p e_y^\top = -2\left(\tilde{C}x + \tilde{D}_p u_p\right)^2 \leq 0 \tag{38}$$

If $x(t)$, $\dot{x}(t)$, and $\dot{r}(t)$ are bounded, then according to the Barbalat's lemma, $\ddot{V}\left(\tilde{C},\tilde{D}\right)$ is bounded. Then, $\dot{V}\left(\tilde{C},\tilde{D}\right) \to 0$ as $t \to \infty$. However, this does not imply that $\tilde{C}(t)$ and $\tilde{D}_p(t)$ tend to zero since $x(t)$ and $u_p(t)$ can be zero signals after some finite time interval. Thus, the persistent excitation condition

$$\frac{1}{T}\int_t^{t+T} \begin{bmatrix} x \\ u_p \end{bmatrix} \begin{bmatrix} x & u_p \end{bmatrix} d\tau \geq \alpha I \tag{39}$$

for all $t \geq t_0$ and some $\alpha > 0$, must be satisfied in order for $\tilde{C}(t) \to 0$ and $\tilde{D}_p(t) \to 0$ exponentially as $t \to \infty$.

If the persistent excitation condition is satisfied, then

$$\dot{V}\left(\tilde{C},\tilde{D}\right) \leq -\frac{2\alpha V\left(\tilde{C},\tilde{D}\right)}{\lambda_{max}\left(\text{diag}\left(\Gamma_c,\Gamma_{D_p}\right)\right)} \tag{40}$$

This yields

$$\left\|\tilde{C}\right\| \leq \sqrt{\frac{V_0}{\lambda_{min}\left(\Gamma_C^{-1}\right)}} \exp\left(-\frac{\alpha t}{\lambda_{max}\left(\text{diag}\left(\Gamma_c,\Gamma_{D_p}\right)\right)}\right) \tag{41}$$

$$\left\|\tilde{D}_p\right\| \leq \sqrt{\frac{V_0}{\lambda_{min}\left(\Gamma_{D_p}^{-1}\right)}} \exp\left(-\frac{\alpha t}{\lambda_{max}\left(\text{diag}\left(\Gamma_c,\Gamma_{D_p}\right)\right)}\right) \tag{42}$$

Therefore, $\tilde{C}(t)$ and $\tilde{D}_p(t)$ converge exponentially to zero as $t \to \infty$ if the persistent excitation condition is satisfied.

■

The closed-loop plant with the performance optimizing controller $u_p(t)$ now becomes

$$\dot{x} = A_m x + B_m r + B_p\bar{K}_x x + B_p\bar{K}_r r - B_a u_{ad} + B_a\Theta_a^{*\top}\Phi(x) \tag{43}$$

If the adaptive controller $u_{ad}(t)$ is designed to achieve the original reference model in Eq. (10), then the effect of the performance optimizing controller $u_p(t)$ represents an unmatched uncertainty that $u_{ad}(t)$ has to reduce. In so doing, the effect of the performance optimizing controller $u_p(t)$ is offset by the adaptive controller $u_{ad}(t)$ and the benefit of the performance optimizing controller $u_p(t)$ would not be realized. Therefore, the reference model must be modified accordingly.

If the parameter convergence is achieved, then the ideal closed-loop plant is expressed as

$$\dot{x} = \left(A_m + B_p\bar{K}_x^*\right)x + \left(B_m + B_p\bar{K}_r^*\right)r - B_a u_{ad} + B_a\Theta_a^{*\top}\Phi(x) \tag{44}$$

Suppose we define the ideal performance optimizing reference model as

$$\dot{x}_m = A_m^* x_m + B_m^* r \tag{45}$$

where $A_m^* = A_m + B_p\bar{K}_x^*$ and $B_m^* = B_m + B_p\bar{K}_r^*$ are pre-computed from the previous optimal control solution. Note that the ideal closed-loop matrix A_m^* is Hurwitz by the property of the optimal control.

Let $\hat{x}_m(t)$ be the estimate of $x_m(t)$. Then,

$$\dot{\hat{x}}_m = \left(A_m + B_p\bar{K}_x\right)\hat{x}_m + \left(B_m + B_p\bar{K}_r\right)r \tag{46}$$

where $\bar{K}_x(t)$ and $\bar{K}_r(t)$ are estimates of $\bar{K}_x^*$ and $\bar{K}_r^*$, respectively, and are computed from Eqs. (29) and (30). Note that the closed-loop matrix $(A_m + B_p\bar{K}_x)$ is Hurwitz by the property of the optimal control.

Let $e(t) = \hat{x}_m(t) - x(t)$ be the tracking error. The adaptive controller is designed as

$$u_{ad} = B_a\Theta_a^\top \Phi(x) \tag{47}$$

Then, the tracking error equation is obtained as

$$\dot{e} = (A_m + B_p\bar{K}_x)e + B_a\tilde{\Theta}_a^\top \Phi(x) \tag{48}$$

$\Theta_a(t)$ is computed by the standard MRAC update law

$$\dot{\Theta}_a = -\Gamma\Phi(x)e^\top WB_a \tag{49}$$

or the optimal control modification adaptive law[9,10]

$$\dot{\Theta}_a = -\Gamma\Phi(x)\left[e^\top W - \nu\Phi^\top(x)\Theta_a B_a^\top W(A_m + B_p\bar{K}_x)^{-1}\right]B_a \tag{50}$$

where $W(t)$ is the solution of the time-varying Ricatti equation (22).

The stability of the MRAC update law can be shown in the following proof:

Proof: Choose a Lyapunov candidate function

$$V(e,\tilde{\Theta}_a) = e^\top We + \text{trace}\left(\tilde{\Theta}_a^\top\Gamma^{-1}\tilde{\Theta}_a\right) \tag{51}$$

Then, $\dot{V}(e,\tilde{\Theta}_a)$ is evaluated as

$$\dot{V}(e,\tilde{\Theta}_a) = e^\top\left(WA_m + WB_p\bar{K}_x + A_m^\top W + \bar{K}_x^\top B_p^\top W\right)e + 2e^\top WB_a\tilde{\Theta}_a^\top\Phi(x) - 2\text{trace}\left(\tilde{\Theta}_a^\top\Phi(x)e^\top WB_a\right) \tag{52}$$

Substituting Eq. (29) into $\dot{V}(e,\tilde{\Theta}_a)$ yields

$$\dot{V}(e,\tilde{\Theta}_a) = e^\top\left(W\bar{A} + \bar{A}^\top W - 2WB_p\bar{R}^{-1}B_p^\top W\right)e = -e^\top\left(\bar{Q} + WB_p\bar{R}^{-1}B_p^\top W\right)e \tag{53}$$

Thus, $\dot{V}(e,\tilde{\Theta}_a)$ is bounded by

$$\dot{V}(e,\tilde{\Theta}_a) \le -\inf\lambda_{min}\left(\bar{Q} + WB_p\bar{R}^{-1}B_p^\top W\right)\|e\|^2 \le 0 \tag{54}$$

Since $\dot{V}(e,\tilde{\Theta}_a) \le 0$, the closed-loop matrix $(A_m + B_p\bar{K}_x)$ is Hurwitz. Then, $e(t) \in \mathscr{L}_2 \cup \mathscr{L}_\infty$ and $\tilde{\Theta}_a(t) \in \mathscr{L}_\infty$. It can be shown that $\ddot{V}(e,\tilde{\Theta}_a)$ is bounded. Then, according to the Barbalat's lemma, $\dot{V}(e,\tilde{\Theta}_a) \to 0$ which implies $e(t) \to 0$ as $t \to \infty$.

■

The optimal control modification adaptive law can be shown to achieve uniform ultimate boundedness in the following proof:

Proof: For the same Lyapunov candidate function in Eq. (51), we evaluate $\dot{V}(e,\tilde{\Theta}_a)$ as

$$\begin{aligned}\dot{V}(e,\tilde{\Theta}_a) &= -e^\top\left(\bar{Q} + WB_p\bar{R}^{-1}B_p^\top W\right)e - 2\nu\text{trace}\left(\tilde{\Theta}_a^\top\Phi(x)\Phi^\top(x)\Theta_a B_a^\top W(A_m + B_p\bar{K}_x)^{-1}B_a\right)\\ &= -e^\top\left(\bar{Q} + WB_p\bar{R}^{-1}B_p^\top W\right)e - 2\nu\Phi^\top(x)\tilde{\Theta}_a B_a^\top W(A_m + B_p\bar{K}_x)^{-1}B_a\tilde{\Theta}_a^\top\Phi(x)\\ &\quad - 2\nu\Phi^\top(x)\Theta_a^* B_a^\top W(A_m + B_p\bar{K}_x)^{-1}B_a\tilde{\Theta}_a^\top\Phi(x)\end{aligned} \tag{55}$$

But

$$W(A_m + B_p\bar{K}_x)^{-1} = M + N \tag{56}$$

where

$$M = \frac{1}{2}W\left(A_m + B_p\bar{K}_x\right)^{-1} + \frac{1}{2}\left(A_m + B_p\bar{K}_x\right)^{-\top}W \tag{57}$$

$$N = \frac{1}{2}W\left(A_m + B_p\bar{K}_x\right)^{-1} - \frac{1}{2}\left(A_m + B_p\bar{K}_x\right)^{-\top}W \tag{58}$$

Then,

$$\begin{aligned}2\left(A_m + B_p\bar{K}_x\right)^{\top}M\left(A_m + B_p\bar{K}_x\right) = \left(A_m + B_p\bar{K}_x\right)^{\top}W + W\left(A_m + B_p\bar{K}_x\right) = W\bar{A} + \bar{A}^{\top}W - 2WB_p\bar{R}^{-1}B_p^{\top}W \\ = -\left(\bar{Q} + WB_p\bar{R}^{-1}B_p^{\top}W\right)\end{aligned} \tag{59}$$

Note that $B_a^{\top}NB_a = 0$ since N is a skew-symmetric matrix. Thus,

$$B_a^{\top}W\left(A_m + B_p\bar{K}_x\right)^{-1}B_a = B_a^{\top}MB_a = -\frac{1}{2}B_a^{\top}\left(A_m + B_p\bar{K}_x\right)^{-\top}\left(\bar{Q} + WB_p\bar{R}^{-1}B_p^{\top}W\right)\left(A_m + B_p\bar{K}_x\right)^{-1}B_a < 0 \tag{60}$$

Then, $\dot{V}\left(e, \tilde{\Theta}_a\right)$ is bounded by

$$\begin{aligned}\dot{V}\left(e, \tilde{\Theta}_a\right) \leq -\lambda_{min}\left(\bar{Q} + WB_p\bar{R}^{-1}B_p^{\top}W\right)\|e\|^2 \\ - \nu\lambda_{min}\left(B_a^{\top}\left(A_m + B_p\bar{K}_x\right)^{-\top}\left(\bar{Q} + WB_p\bar{R}^{-1}B_p^{\top}W\right)\left(A_m + B_p\bar{K}_x\right)^{-1}B_a\right)\|\Phi(x)\|^2\left\|\tilde{\Theta}_a\right\|^2 \\ + 2\nu\left\|B_a^{\top}W\left(A_m + B_p\bar{K}_x\right)^{-1}B_a\right\|\|\Phi(x)\|^2\left\|\tilde{\Theta}_a\right\|\|\Theta_a^*\|\end{aligned} \tag{61}$$

Upon completing the square, we have

$$\dot{V}\left(e, \tilde{\Theta}_a\right) \leq -c_1\|e\|^2 - \nu c_2\|\Phi(x)\|^2\left(\left\|\tilde{\Theta}_a\right\| - c_3\right)^2 + \nu c_2 c_3^2\|\Phi(x)\|^2 \tag{62}$$

where $c_1 = \inf\lambda_{min}\left(\bar{Q} + WB_p\bar{R}^{-1}B_p^{\top}W\right) > 0$, $c_2 = \inf\lambda_{min}\left(B_a^{\top}\left(A_m + B_p\bar{K}_x\right)^{-\top}\left(\bar{Q} + WB_p\bar{R}^{-1}B_p^{\top}W\right)\left(A_m + B_p\bar{K}_x\right)^{-1}B_a\right) > 0$, and $c_3 = \frac{\sup\left\|B_a^{\top}W\left(A_m + B_p\bar{K}_x\right)^{-1}B_a\right\|\|\Theta_a^*\|}{c_2} > 0$.

Thus, $\dot{V}\left(e, \tilde{\Theta}_a\right) \leq 0$ implies

$$\|e\| \geq \sqrt{\frac{\nu c_2 c_3^2\|\Phi(x)\|^2}{c_1}} = p \tag{63}$$

$$\left\|\tilde{\Theta}_a\right\| \geq 2c_3 = \alpha \tag{64}$$

Let $\varphi\left(\|x\|, \|x_m\|, \|\Theta_a^*\|, \nu, \bar{Q}, \bar{R}\right)$ be the largest upper bound of $\dot{V}\left(e, \tilde{\Theta}_a\right)$ such that $\dot{V}\left(e, \tilde{\Theta}_a\right) \leq \varphi$ where

$$\varphi\left(\|x\|, \|x_m\|, \|\Theta_a^*\|, \nu, \bar{Q}, \bar{R}\right) = -c_1\|x\|^2 + 2c_4\|x\|\|x_m\| - c_1\|x_m\|^2 + \nu c_2 c_3^2\|\Phi(x)\|^2 \tag{65}$$

with $c_4 = \sup\lambda_{max}\left(\bar{Q} + WB_p\bar{R}^{-1}B_p^{\top}W\right) > 0$.

Then, for any $0 < \nu < \nu_{max}$, $\|x\|$ can be determined by

$$\|x\| = \varphi^{-1}\left(\|x_m\|, \|\Theta_a^*\|, \nu, \bar{Q}, \bar{R}\right) \tag{66}$$

It follows that $\|\Phi(x)\|$ is bounded by

$$\|\Phi(x)\| \leq \left\|\Phi\left(\varphi^{-1}\left(\|x_m\|, \|\Theta_a^*\|, \nu, \bar{Q}, \bar{R}\right)\right)\right\| = \Phi_0 \tag{67}$$

Then, the closed-loop system is uniformly ultimately bounded with the following ultimate bounds:

$$\|e\| \leq \sqrt{\frac{\sup\lambda_{max}(W)\,p^2 + \lambda_{max}\left(\Gamma^{-1}\right)\alpha^2}{\inf\lambda_{min}(W)}} \tag{68}$$

$$\left\|\tilde{\Theta}_a\right\| \leq \sqrt{\frac{\sup\lambda_{max}(W)\,p^2 + \lambda_{max}\left(\Gamma^{-1}\right)\alpha^2}{\lambda_{min}\left(\Gamma^{-1}\right)}} \tag{69}$$

III. Application

In the recent years, NASA has developed a new type of aircraft flight control surfaces called the Variable Camber Continuous Trailing Edge Flap (VCCTEF).[11–14] The VCCTEF, illustrated in Fig. 1, developed by Nguyen is a wing shaping control device designed to reshape a flexible aircraft wing in-flight to improve the aerodynamic performance while suppressing any adverse aeroelastic interactions. It employs three chordwise flap segments to provide a variable camber to change the wing shape for increasing the aerodynamic performance. The flap is also made up of individual spanwise sections which enable different flap settings at each flap spanwise position. This results in the ability to control the wing shape as a function of the wing span, thereby resulting in a change to the wing twist to establish the best lift-to-drag ratio at any aircraft gross weight or mission segment. The individual spanwise flap sections are connected with a flexible elastomer material to form a continuous trailing edge with no flap gaps in the wing planform for drag and noise reduction purposes.

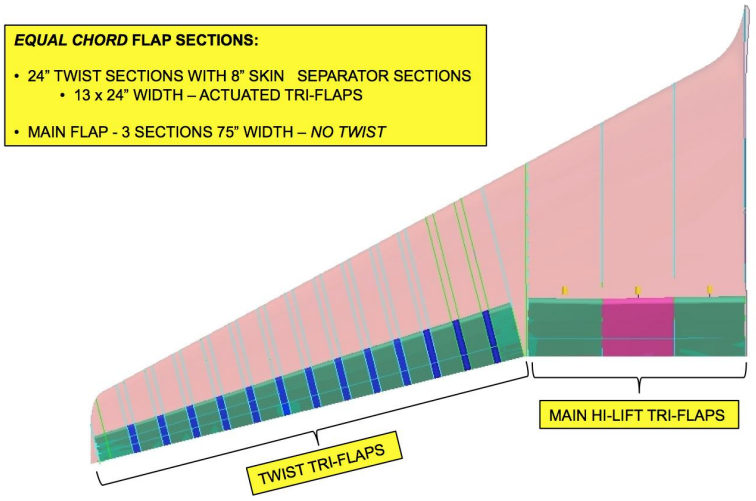

Figure 1. Variable Camber Continuous Trailing Edge Flap (VCCTEF)

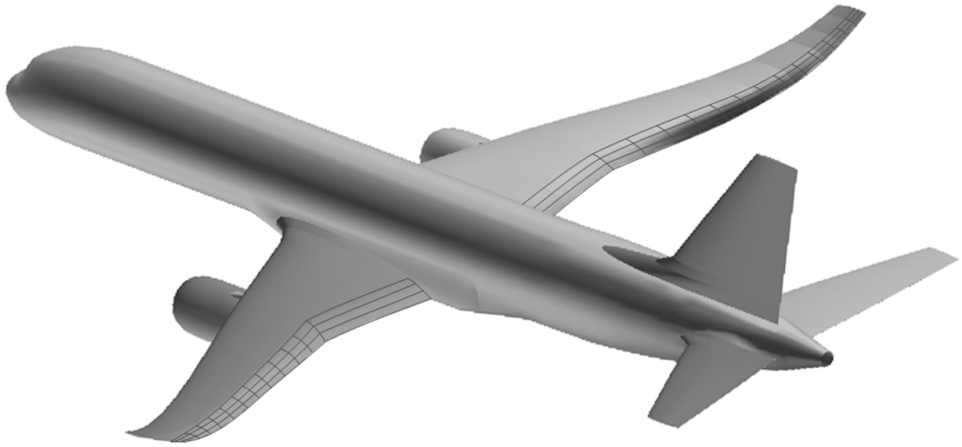

Figure 2. GTM with with Variable Camber Continuous Trailing Edge Flap

The VCCTEF are multi-functional flight control surfaces designed for drag minimization, flutter suppression, and load alleviation. For the application, we conduct simulations of a flexible wing Generic Transport Model (GTM) equipped with the VCCTEF as shown in Fig. 2. One of the performance objectives is to reduce structural loads on the aircraft wings during maneuvers. Aircraft wings are designed to meet certain load factors, typically 2.5 times the aircraft weight for transport aircraft. The availability of the VCCTEF allows the wing lift distribution to be re-distributed for maneuver load alleviation control which is viewed as a performance optimizing control objective. A pull-up maneuver is simulated with the VCCTEF deployed for maneuver load alleviation while the elevator is deployed for pitch rate control.

Consider a linearized model of a flexible aircraft with matched uncertainty

$$\dot{x} = Ax + B\left[u - \Theta^{*\top}\Phi(x_r)\right] \tag{70}$$

where $x(t) \in \mathbb{R}^n$ is a state vector that is composed of a rigid aircraft state vector $x_r(t) \in \mathbb{R}^{n_r}$ and an elastic wing state vector $x_e(t) \in \mathbb{R}^{n_e=n-n_r}$, $u(t) \in \mathbb{R}^m$ is a control vector, $A \in \mathbb{R}^{n\times n}$ and $B \in \mathbb{R}^{n\times m}$ are constant and known matrices, and $\Theta^* \in \mathbb{R}^{p\times m}$ is a constant and unknown matrix that represents a matched parametric uncertainty in the rigid aircraft state, and $\Phi(x_r) \in \mathbb{R}^p$ is a vector of known regressors.

The performance metric is the wing root bending moment due to the wing lift distribution which is given by

$$y = Cx + Du \tag{71}$$

where $y(t) \in \mathbb{R}$ is a measured output, and $C \in \mathbb{R}^n$ and $D \in \mathbb{R}^m$ are unknown constant matrices.

Assuming that there is a sufficient frequency separation between the "slow" rigid aircraft dynamics and "fast" elastic wing dynamics. Then, the fast and slow dynamics can be decoupled using the standard singular perturbation method. The fast dynamics of the elastic wing modes are assumed to approach the equilibrium solution infinitely fast. Therefore, the rigid aircraft dynamics with approximately zero-order elastic wing dynamics can be obtained by setting $\dot{x}_e(t) = \varepsilon(x)$ where ε is a small parameter.[15] Thus, the state-space model can be expressed in a component form as

$$\begin{bmatrix} \dot{x}_r \\ \varepsilon \end{bmatrix} = \begin{bmatrix} A_{rr} & A_{re} \\ A_{er} & A_{ee} \end{bmatrix} \begin{bmatrix} x_r \\ x_e \end{bmatrix} + \begin{bmatrix} B_{rp} & B_a \\ B_{ep} & 0 \end{bmatrix} \begin{bmatrix} u_p \\ u_a + \Theta^{*\top}\Phi(x_r) \end{bmatrix} \tag{72}$$

where $u_p(t) \in \mathbb{R}^{m-1}$ is a control input vector due to the VCCTEF and $u_a(t) \in \mathbb{R}$ is a control input due to the elevator.

Then, the elastic wing dynamics are approximated by

$$x_e = A_{ee}^{-1}\varepsilon(x) - A_{ee}^{-1}A_{er}x_r - A_{ee}^{-1}B_{ep}u_p \tag{73}$$

Substituting $x_e(t)$ into the rigid aircraft dynamics yields

$$\dot{x}_r = A_r x_r + B_p u_p + B_a\left[u_a - \Theta^{*\top}\Phi(x_r)\right] + \Delta(x) \tag{74}$$

where

$$A_r = A_{rr} - A_{re}A_{ee}^{-1}A_{er} \tag{75}$$

$$B_p = B_{rp} - A_{re}A_{ee}^{-1}B_{ep} \tag{76}$$

$$\Delta(x) = A_{re}A_{ee}^{-1}\varepsilon(x) \tag{77}$$

The term $\Delta(x)$ represents the effect of unmodeled dynamics of the elastic wing modes. The reduced-order plant matrix A_r is assumed to be Hurwitz.

The output $y(t)$is expressed in a component form as

$$y = \begin{bmatrix} C_{yr} & C_{ye} \end{bmatrix} \begin{bmatrix} x_r \\ x_e \end{bmatrix} + \begin{bmatrix} D_{yp} & 0 \end{bmatrix} \begin{bmatrix} u_p \\ u_a \end{bmatrix} \tag{78}$$

The reduced-order output is then obtained as

$$y = C_r x_r + D_p u_p + \delta(x) \tag{79}$$

where

$$C_r = C_{yr} - C_{ye}A_{ee}^{-1}A_{er} \tag{80}$$

$$D_p = D_{yp} - C_{ye}A_{ee}^{-1}B_{ep} \tag{81}$$

$$\delta(x) = C_{ye}A_{ee}^{-1}\varepsilon(x) \tag{82}$$

The performance optimizing controller $u_p(t)$ comprises 16 individual trailing edge flaps, each connected to an adjacent flap by an elastomer transition section show in blue in Fig. 1. Due to the stiffness imposed by the transition section, a constraint on the relative deflection of any two adjacent flaps is imposed on the control input command. In order to address this relative deflection constraint, a virtual control concept is used whereby the actually flap deflection of each flap is mapped into a mathematically smooth shape function whose coefficients are the virtual control variables.[5] A cubic Chebyshev polynomial is selected as a candidate shape function. Then, the flap deflection of the i-th flap is expressed as

$$\delta_i = c_0 + c_1 k + c_2\left(2k^2 - 1\right) + c_3\left(4k^3 - 3k\right) \tag{83}$$

where $k = \frac{i-1}{n-1}$, $i = 1,2,\ldots,16$, $n = 16$, and $c_j(t)$, $j = 0,1,2,3$ are the virtual control variables.

Let $u_p(t) = c(t) = \begin{bmatrix} c_0(t) & c_1(t) & c_2(t) & c_3(t) \end{bmatrix}$ be a vector of the virtual control inputs. Then, the performance optimizing controller $u_p(t)$ is designed as

$$u_p = \bar{K}_{x_r}(t)\,x_r + \bar{K}_r(t)\,r \tag{84}$$

where $\bar{K}_{x_r}(t)$ and $\bar{K}_r(t)$ are to be computed from Eqs. (29) and (30).

The longitudinal rigid aircraft model is given by

$$\begin{bmatrix} \dot{h} \\ \frac{\dot{h}}{\bar{h}} \\ \frac{\dot{V}}{\bar{V}} \\ \dot{\alpha} \\ \dot{q} \\ \dot{\theta} \end{bmatrix} = \begin{bmatrix} 0 & \frac{\bar{V}\bar{\gamma}}{\bar{h}} & -\frac{\bar{V}}{\bar{h}} & 0 & \frac{\bar{V}}{\bar{h}} \\ \frac{X_h\bar{h}}{\bar{V}} + \frac{X_{\dot{\alpha}}Z_h\bar{h}}{\bar{V}^2 - Z_{\dot{\alpha}}\bar{V}} & X_u + \frac{X_{\dot{\alpha}}Z_u}{\bar{V} - Z_{\dot{\alpha}}} & \frac{X_\alpha}{\bar{V}} + \frac{X_{\dot{\alpha}}Z_\alpha}{\bar{V}^2 - Z_{\dot{\alpha}}\bar{V}} & \frac{X_q}{\bar{V}} - \bar{\alpha} + \frac{X_{\dot{\alpha}}\left(Z_q + \bar{V}\right)}{\bar{V}^2 - Z_{\dot{\alpha}}\bar{V}} & -\frac{g}{\bar{V}}\left(1 + \frac{X_{\dot{\alpha}}\bar{\theta}}{\bar{V} - Z_{\dot{\alpha}}}\right) \\ \frac{Z_h\bar{h}}{\bar{V} - Z_{\dot{\alpha}}} & \frac{Z_u\bar{V}}{\bar{V} - Z_{\dot{\alpha}}} & \frac{Z_\alpha}{\bar{V} - Z_{\dot{\alpha}}} & \frac{Z_q - \bar{V}}{\bar{V} - Z_{\dot{\alpha}}} & -\frac{g\bar{\theta}}{\bar{V} - Z_{\dot{\alpha}}} \\ M_h\bar{h} + \frac{M_{\dot{\alpha}}Z_h\bar{h}}{\bar{V} - Z_{\dot{\alpha}}} & M_u\bar{V} + \frac{M_{\dot{\alpha}}Z_u\bar{V}}{\bar{V} - Z_{\dot{\alpha}}} & M_\alpha + \frac{M_{\dot{\alpha}}Z_\alpha}{\bar{V} - Z_{\dot{\alpha}}} & M_q + \frac{M_{\dot{\alpha}}\left(Z_q + \bar{V}\right)}{\bar{V} - Z_{\dot{\alpha}}} & -\frac{M_{\dot{\alpha}}g\bar{\theta}}{\bar{V} - Z_{\dot{\alpha}}} \\ 0 & 0 & 0 & 1 & 0 \end{bmatrix} \begin{bmatrix} \frac{h}{\bar{h}} \\ \frac{V}{\bar{V}} \\ \alpha \\ q \\ \theta \end{bmatrix}$$

$$+ \begin{bmatrix} 0 \\ \frac{X_c}{\bar{V}} \\ \frac{Z_c}{\bar{V} - Z_{\dot{\alpha}}} \\ M_c + \frac{M_{\dot{\alpha}}Z_c}{\bar{V} - Z_{\dot{\alpha}}} \\ 0 \end{bmatrix} c + \begin{bmatrix} 0 \\ \frac{X_{\delta_e}}{\bar{V}} + \frac{X_\alpha Z_{\delta_e}}{\bar{V}^2 - Z_{\dot{\alpha}}\bar{V}} \\ \frac{Z_{\delta_e}}{\bar{V} - Z_{\dot{\alpha}}} \\ M_{\delta_e} + \frac{M_\alpha Z_{\delta_e}}{\bar{V} - Z_{\dot{\alpha}}} \\ 0 \end{bmatrix} \left(\delta_e + \begin{bmatrix} 0 & 0 & \theta_\alpha^* & \theta_q^* & 0 \end{bmatrix} \begin{bmatrix} h \\ V \\ \alpha \\ q \\ \theta \end{bmatrix} \right) + \tag{85}$$

where $h(t)$ is the altitude, $V(t)$ is the airspeed, $\alpha(t)$ is the angle of attack, $q(t)$ is the pitch rate, $\theta(t)$ is the pitch attitude, $\gamma(t)$ is the flight path angle, X is the aircraft axial force, Z is the aircraft normal force, M is the aircraft pitching moment, g is the gravity constant, $\delta(t) \in \mathbb{R}^{m-1}$ is a vector of the VCCTEF deflections, δ_e is the elevator deflection, θ_α^* and θ_q^* represent the matched uncertainty in $\alpha(t)$ and $q(t)$, the subscripts denote the partial derivatives, and the bar symbol denotes the trim values.

Numerically, the rigid aircraft model of the GTM at Mach 0.797 and an altitude of 36,000 ft[7] without the perfor-

mance optimizing controller $u_p(t)$ according to Eq. (72) is given by

$$\begin{bmatrix} \dot{\frac{h}{\bar{h}}} \\ \dot{\frac{V}{\bar{V}}} \\ \dot{\alpha} \\ \dot{q} \\ \dot{\theta} \end{bmatrix} = \begin{bmatrix} 0 & 0 & -0.0214 & 0 & 0.0214 \\ -0.0011 & -0.0132 & -0.0050 & -0.0012 & -0.0417 \\ 0.0584 & -0.1708 & -0.4775 & 0.9883 & -0.0000 \\ -0.0044 & -0.4473 & -1.8402 & -0.3556 & -0.0001 \\ 0 & 0 & 0 & 1 & 0 \end{bmatrix} \begin{bmatrix} \frac{h}{\bar{h}} \\ \frac{V}{\bar{V}} \\ \alpha \\ q \\ \theta \end{bmatrix}$$
$$+ \begin{bmatrix} 0 & 0 & 0 & 0 \\ -0.0074 & -0.0015 & 0.0056 & 0.0019 \\ -0.0783 & -0.0186 & 0.0550 & 0.0218 \\ -0.6742 & -0.2125 & 0.3904 & 0.2059 \\ 0 & 0 & 0 & 0 \end{bmatrix} \begin{bmatrix} c_0 \\ c_1 \\ c_2 \\ c_3 \end{bmatrix} + \begin{bmatrix} 0 \\ -0.0051 \\ -0.0395 \\ -2.3356 \\ 0 \end{bmatrix} \left(\delta_e + \begin{bmatrix} 0 & 0 & -0.5 & -0.4 & 0 \end{bmatrix} \begin{bmatrix} \frac{h}{\bar{h}} \\ \frac{V}{\bar{V}} \\ \alpha \\ q \\ \theta \end{bmatrix} \right)$$

The eigenvalues of the rigid aircraft model are $-0.4224 \pm 1.3477i$, $-0.0002 \pm 0.0573i$, and -0.0010 corresponding to the short period mode, phugoid mode, and rigid body plunge mode, respectively.

The wing root bending moment due to the rigid aircraft model is given by

$$y = 10^7 \begin{bmatrix} -0.0003 & 0.2699 & 2.0943 & 0.0385 & -0.0114 \end{bmatrix} \begin{bmatrix} \frac{h}{\bar{h}} \\ \frac{V}{\bar{V}} \\ \alpha \\ q \\ \theta \end{bmatrix}$$
$$+ 10^6 \begin{bmatrix} 1.5354 & 1.3986 & 0.3776 & -1.2469 \end{bmatrix} \begin{bmatrix} c_0 \\ c_1 \\ c_2 \\ c_3 \end{bmatrix}$$

For comparison, the reduced-order model of the flexible wing GTM according to Eq. (74) is given by

$$\begin{bmatrix} \dot{\frac{h}{\bar{h}}} \\ \dot{\frac{V}{\bar{V}}} \\ \dot{\alpha} \\ \dot{q} \\ \dot{\theta} \end{bmatrix} = \begin{bmatrix} 0 & 0 & -0.0214 & 0 & 0.0214 \\ -0.0011 & -0.0118 & -0.0204 & -0.0015 & -0.0418 \\ 0.0584 & -0.1536 & -0.6687 & 0.9858 & -0.0007 \\ -0.0045 & -0.3426 & -3.2860 & -0.3786 & -0.0045 \\ 0 & 0 & 0 & 1 & 0 \end{bmatrix} \begin{bmatrix} \frac{h}{\bar{h}} \\ \frac{V}{\bar{V}} \\ \alpha \\ q \\ \theta \end{bmatrix}$$
$$+ \begin{bmatrix} 0 & 0 & 0 & 0 \\ -0.0062 & -0.0002 & 0.0061 & 0.0009 \\ -0.0648 & -0.0046 & 0.0611 & 0.0104 \\ -0.6720 & -0.0946 & 0.5605 & 0.1295 \\ 0 & 0 & 0 & 0 \end{bmatrix} \begin{bmatrix} c_0 \\ c_1 \\ c_2 \\ c_3 \end{bmatrix} + \begin{bmatrix} 0 \\ -0.0051 \\ -0.0395 \\ -2.3356 \\ 0 \end{bmatrix} \left(\delta_e + \begin{bmatrix} 0 & 0 & -0.5 & -0.4 & 0 \end{bmatrix} \begin{bmatrix} \frac{h}{\bar{h}} \\ \frac{V}{\bar{V}} \\ \alpha \\ q \\ \theta \end{bmatrix} \right) + \Delta(x)$$

The eigenvalues of the reduced-order model are $-0.5273 \pm 1.7943i$, $-0.0013 \pm 0.0669i$, and -0.0018 corresponding to the short period mode, phugoid mode, and rigid body plunge mode, respectively.

The reduced-order model of the wing root bending moment is given by

$$y = 10^7 \begin{bmatrix} -0.0002 & 0.1492 & 3.6333 & 0.0615 & -0.0063 \end{bmatrix} \begin{bmatrix} \frac{h}{\bar{h}} \\ \frac{V}{\bar{V}} \\ \alpha \\ q \\ \theta \end{bmatrix} + 10^6 \begin{bmatrix} 1.1554 & 0.1961 & -0.9749 & -0.4012 \end{bmatrix} \begin{bmatrix} c_0 \\ c_1 \\ c_2 \\ c_3 \end{bmatrix} + \delta(x)$$

We design a pitch attitude controller using the reduced-order model to track the following second-order pitch attitude reference model:

$$\ddot{\theta}_m + 2\zeta\omega_n\dot{\theta}_m + \omega_n^2\theta_m = \omega_n^2 r \tag{86}$$

where $\zeta = \frac{1}{\sqrt{2}}$ is chosen to be the closed-loop damping ratio and $\omega_n = 1.5$ rad/sec is chosen to be the closed-loop frequency.

The nominal controller is designed as

$$u_{nom} = k_h\frac{h}{\bar{h}} + k_V\frac{V}{\bar{V}} + k_\alpha\alpha + k_q q + k_\theta\theta + k_r r \tag{87}$$

Then, the closed-loop pitch attitude dynamics become

$$\ddot{\theta} = \left(M_h\bar{h} + \frac{M_\alpha Z_h\bar{h}}{\bar{V} - Z_{\dot{\alpha}}}\right)\frac{h}{\bar{h}} + \left(M_u\bar{V} + \frac{M_\alpha Z_u\bar{V}}{\bar{V} - Z_{\dot{\alpha}}}\right)\frac{V}{\bar{V}} + \left(M_\alpha + \frac{M_\alpha Z_\alpha}{\bar{V} - Z_{\dot{\alpha}}}\right)\alpha + \left[M_q + \frac{M_{\dot{\alpha}}(Z_q + \bar{V})}{\bar{V} - Z_{\dot{\alpha}}}\right]q - \frac{M_{\dot{\alpha}}g\bar{\theta}}{\bar{V} - Z_{\dot{\alpha}}}\theta + \left(M_{\delta_e} + \frac{M_{\dot{\alpha}}Z_{\delta_e}}{\bar{V} - Z_{\dot{\alpha}}}\right)(k_h h + k_V V + k_\alpha\alpha + k_q q + k_\theta\theta + k_r r) \tag{88}$$

Matching the closed-loop dynamics with the reference model yields

$$k_h = -\frac{M_h\bar{h}(\bar{V} - Z_{\dot{\alpha}}) + M_{\dot{\alpha}}Z_h\bar{h}}{M_{\delta_e}(\bar{V} - Z_{\dot{\alpha}}) + M_{\dot{\alpha}}Z_{\delta_e}} \tag{89}$$

$$k_V = -\frac{M_u\bar{V}(\bar{V} - Z_{\dot{\alpha}}) + M_{\dot{\alpha}}Z_u\bar{V}}{M_{\delta_e}(\bar{V} - Z_{\dot{\alpha}}) + M_{\dot{\alpha}}Z_{\delta_e}} \tag{90}$$

$$k_\alpha = -\frac{M_\alpha(\bar{V} - Z_{\dot{\alpha}}) + M_{\dot{\alpha}}Z_\alpha}{M_{\delta_e}(\bar{V} - Z_{\dot{\alpha}}) + M_{\dot{\alpha}}Z_{\delta_e}} \tag{91}$$

$$k_q = -\frac{(2\zeta\omega_n + M_q)(\bar{V} - Z_{\dot{\alpha}}) + M_{\dot{\alpha}}(Z_q + \bar{V})}{M_{\delta_e}(\bar{V} - Z_{\dot{\alpha}}) + M_{\dot{\alpha}}Z_{\delta_e}} \tag{92}$$

$$k_\theta = -\frac{\omega_n^2(\bar{V} - Z_{\dot{\alpha}}) - M_{\dot{\alpha}}g\bar{\theta}}{M_{\delta_e}(\bar{V} - Z_{\dot{\alpha}}) + M_{\dot{\alpha}}Z_{\delta_e}} \tag{93}$$

$$k_r = \frac{\omega_n^2(\bar{V} - Z_{\dot{\alpha}})}{M_{\delta_e}(\bar{V} - Z_{\dot{\alpha}}) + M_{\dot{\alpha}}Z_{\delta_e}} \tag{94}$$

This results in $K_{x_r} = \begin{bmatrix} k_h & k_V & k_\alpha & k_q & k_\theta \end{bmatrix} = \begin{bmatrix} -0.0019 & -0.1467 & -1.4069 & 0.7462 & 0.9614 \end{bmatrix}$ and $k_r = -0.9633$. The closed-loop plant is selected as a reference model defined by

$$\dot{x}_m = A_m x_m + B_m r \tag{95}$$

where

$$A_m = A_r + B_a K_{x_r} = \begin{bmatrix} 0 & 0 & -0.0214 & 0 & 0.0214 \\ -0.0011 & -0.0111 & -0.0133 & -0.0052 & -0.0466 \\ 0.0585 & -0.1478 & -0.6132 & 0.9563 & -0.0387 \\ 0 & 0 & 0 & -2.1213 & -2.2500 \\ 0 & 0 & 0 & 1 & 0 \end{bmatrix}$$

$$B_m = B_a k_r = \begin{bmatrix} 0 \\ 0.0049 \\ 0.0380 \\ 2.2500 \\ 0 \end{bmatrix}$$

The eigenvalues of the reduced-order model are $-1.0607 \pm 1.0607i$, $-0.0049 \pm 0.0020i$, and -0.6144 corresponding to the short period mode, phugoid mode, and rigid body plunge mode, respectively.

We initially choose a sinusoidal reference command signal $r(t) = \theta_0 \sin \omega t$ where $\theta_0 = 20^\circ$ and $\omega = 2$ rad/sec to ensure the persistently exciting signal quality for parameter convergence. The simulation include a full flexible 10 flexible modes each with 2 elastic states and 4 aerodynamic lag states for the unsteady aerodynamic approximation. Thus, the full model has a total of 65 states. The performance optimizing weighting coefficient is selected to be $q = 6 \times 10^{-12}$. The control weighting matrix is selected to be $R = 2000I$. The unknown matrices $\Theta(t)$ $\hat{C}(t)$ and $\hat{D}(t)$ are all initialized with zero values. The adaptation rates are chosen to be $\Gamma = \text{diag}(0,0,0.2,1,0)$, $\Gamma_C = \text{diag}(10,5000,1000,5,1)$, and $\Gamma_{D_p} = \text{diag}(40,40,40,70)$. The optimal control modification adaptive law is implemented with $\nu = 0.01$. The solution of the time-varying Ricatti equation is computed on-line at each time step.

Figure 3 shows the response of the aircraft. The red curves are the initial or baseline reference model signals without the performance optimizing adaptive controller, denoted with the asterisk superscript. The blue curves are the rigid aircraft states and the green curves are the states of the time-varying modified reference model signals with the performance adaptive controller. The aircraft response tracks the time-varying modified reference model very well. The signals with the performance optimizing adaptive controller are reduced in amplitudes from the signals without the performance optimizing adaptive controller. In particular, the performance metric $y(t)$, which is the wing root bending moment also shown in Fig. 3, is reduced in amplitude by the performance optimizing adaptive controller from the bending moment with the original reference model. The 23.5% reduction in the wing root bending moment thus validates the performance optimization goal of the adaptive controller. The estimated performance metric $\hat{y}(t)$ converges to the actual measured performance metric $y(t)$ extremely well. Reducing the control weighting matrix R will increase the wing root bending moment reduction but the control surface deflections of the VCCTEF increase and can potentially violate the relative deflection constraint or the position limit.

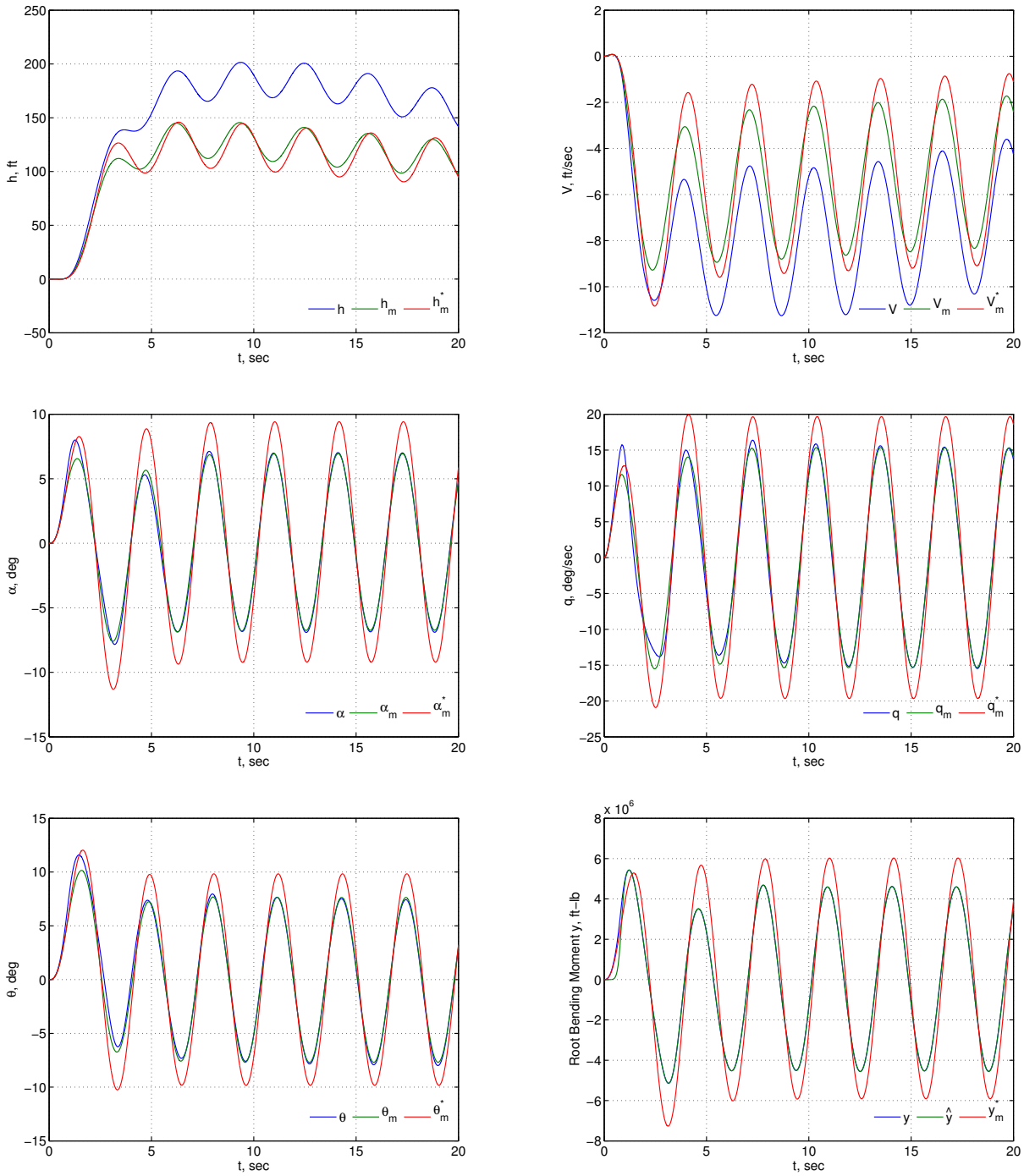

Figure 3. Aircraft Response to Performance Optimizing Adaptive Control with $r(t) = \theta_0 \sin \omega t$

Figure 4 shows the control signals of the elevator and the VCCTEF deflections. All the control signals look well-behaved. The VCCTEF deflections are rather large during the initial transients.

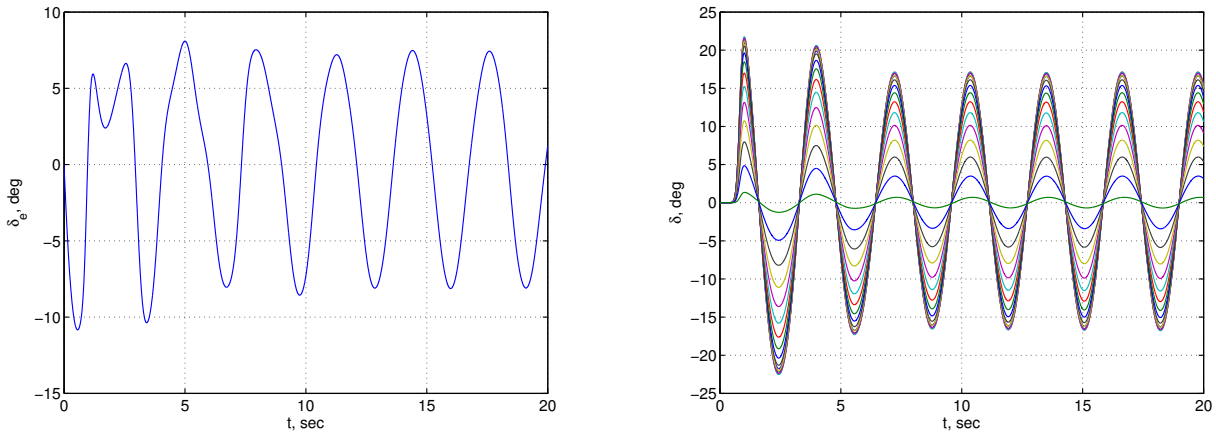

Figure 4. Control Signals of Performance Optimizing Adaptive Control with $r(t) = \theta_0 \sin \omega t$

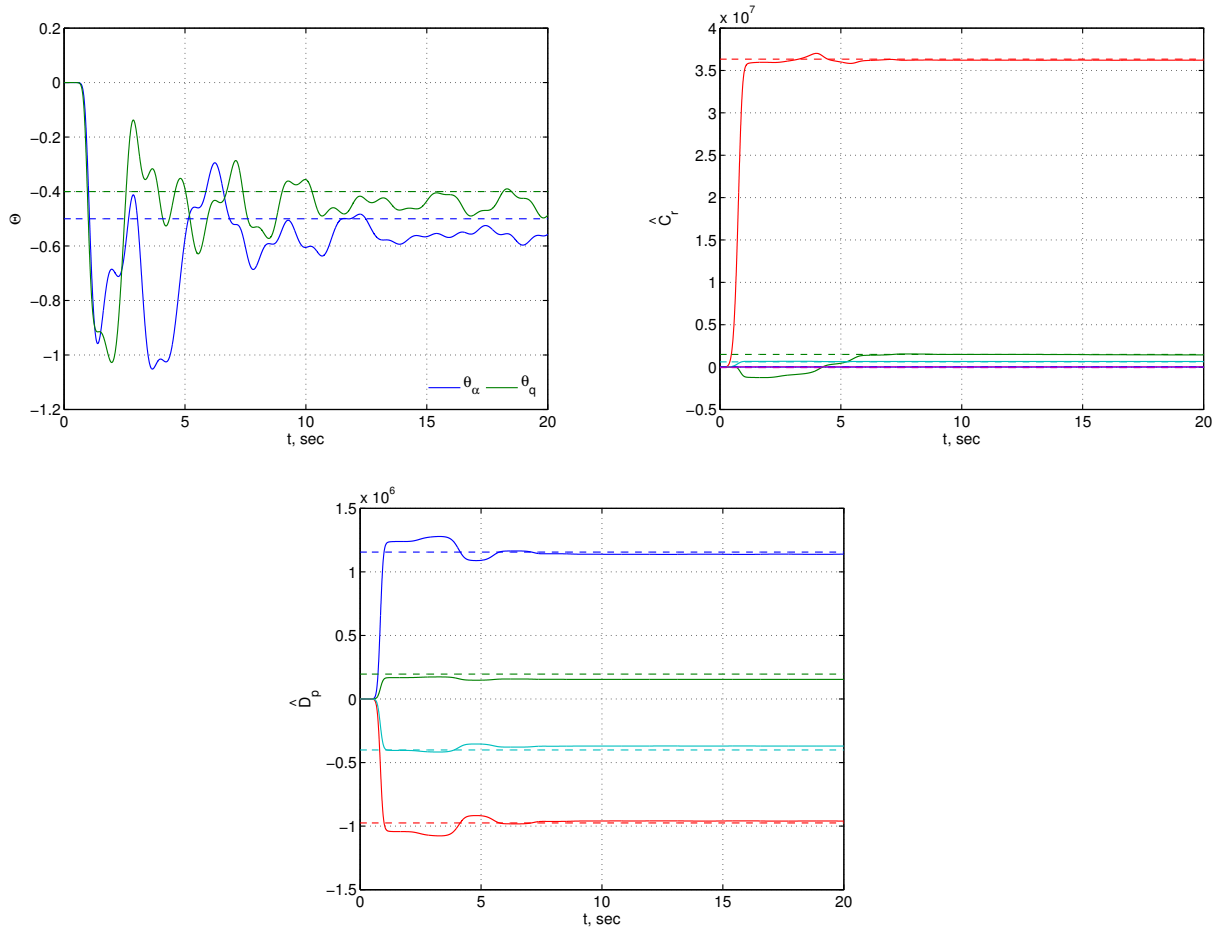

Figure 5. Time Histories of Adaptive Parameters $\Theta(t)$, $\hat{C}_r$, and $\hat{D}_p$

Figure 5 shows the time histories of the adaptive parameters $\Theta(t)$, $\hat{C}_r(t)$, and $\hat{D}_p(t)$. The elements of the estimated matrices $\hat{C}_r(t)$ and $\hat{D}_p(t)$ converge very rapidly after 6 sec to their steady state values close to the true values. The elements of $\Theta(t)$ do not converge but fluctuate near their ideal values. The optimal control modification reduces initial high frequency oscillations in the signals.

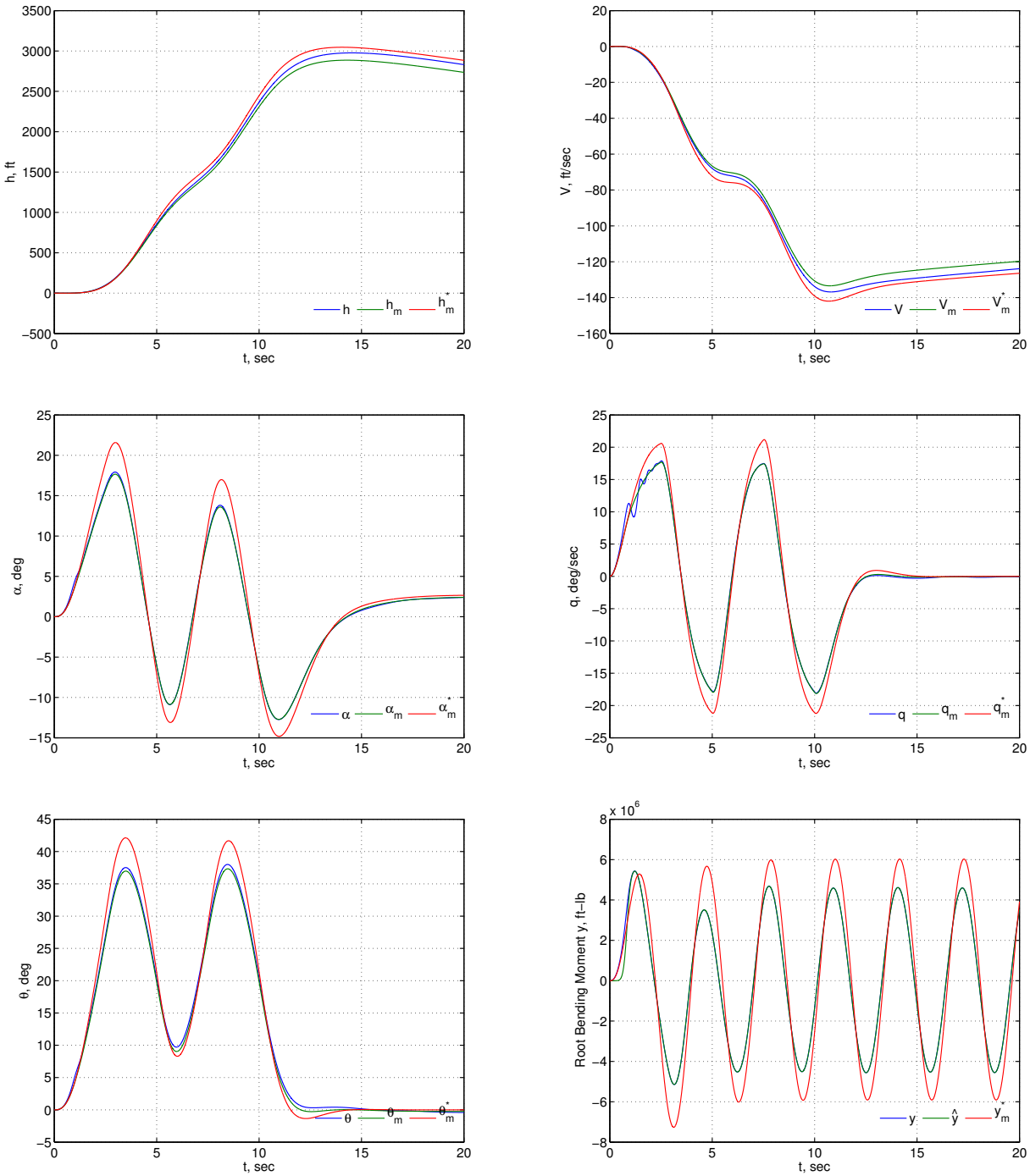

Figure 6. Aircraft Response to Performance Optimizing Adaptive Control for Pull-Up Maneuver

A more realistic simulation of a sharp pull-up maneuver is conducted with a pitch rate doublet input of more than 20°/sec during the first 12 sec. The pitch rate is then held at zero thereafter. The performance optimizing weighting coefficient is selected to be $q = 6 \times 10^{-12}$. The control weighting matrix is selected to be $R = 5000I$. The adaptation rates are chosen to be $\Gamma = \text{diag}\,(0,0,1,1,0)$, $\Gamma_C = \text{diag}\,(10,10000,2000,5,1)$, and $\Gamma_{D_p} = \text{diag}\,(150,150,150,300)$. The optimal control modification adaptive law is implemented with $\nu = 0.01$.

Figure 6 shows the response of the aircraft during the pull-up maneuver. The altitude increases rapidly to about 3000 ft after 13 sec. At the same time, the airspeed drops by 140 ft/sec at 10 sec. The pitch rate increases rapidly to 20° which results in a pitch angle of as high as 42°. Without the performance optimizing adaptive control, the angle of attack increases rapidly to 21.6° which most likely would result in an aircraft stall. The performance optimizing adaptive controller brings the angle of attack down to 17.7°, a decrease of 18.2%. As a result, the wing root bending moment decreases by 14.4%. Reducing the control weighting matrix R can further reduce the angle of attack and the wing root bending moment, but will increase the VCCTEF deflections which could potentially violate the relative deflection constraint or the position limit.

Figure 7 shows the control signals of the elevator and the VCCTEF deflections. All the control signals look well-behaved. The VCCTEF deflections are rather large during the initial transients. This is necessary for the maneuver load alleviation. Increasing the VCCTEF deflections can further reduce the angle of attack and the wing root bending moment.

It is noted that the performance optimizing adaptive controller seems to be quite robust. The selection of the adaptation rates influence the parameter convergence. Even though the parameters may not converge, good performance in terms of the maneuver load alleviation is still attained. The computation of the time-varying solution of the Ricatti equation to modify the reference model slows down the simulations significantly. It may be possible to implement a real-time solution method for the time-varying Ricatti equation in a control hardware system on a modern computer.

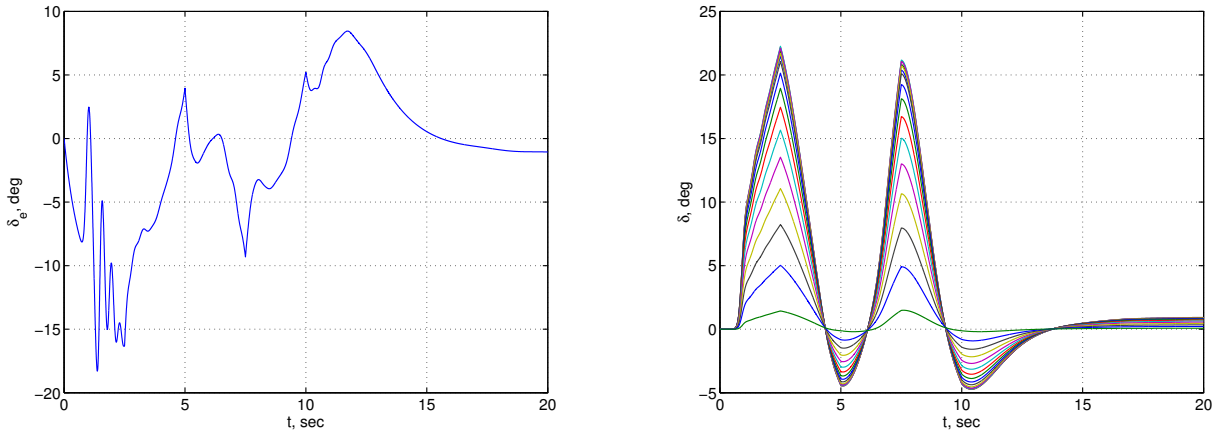

Figure 7. Control Signals of Performance Optimizing Adaptive Control for Pull-Up Maneuver

IV. Conclusions

This paper presents a new method that addresses a real-time optimization of a performance metric in the context of adaptive control. This approach is called performance optimizing adaptive control. The plant has two sets of control inputs. One set of the control inputs provides the normal plant adaptation to cancel the matched uncertainty to follow an initial reference model which has no notion of performance optimization. The second set of the control inputs is dedicated to the performance optimization of the plant. The plant is assumed to have measurements of the performance metric which has unknown state and control sensitivities. The performance optimization is formulated as a multi-objective optimal control problem coupled with a least-squares adaptive law for estimating the unknown sensitivities of the performance metric needed for the optimal control. This results in a time-varying Ricatti equation

whose solution provides time-varying control gains for use in time-varying modified reference model. The Lyapunov stability theory shows that the model-reference adaptive control with the time-varying modified reference model to achieve the performance optimization is stable and bounded. Simulations of a maneuver load alleviation control show the effectiveness of the time-varying modified reference model and the reduction in the wing root bending moment.

References

[1]Nguyen, N., Swei, S., and Ting, E., "Adaptive Linear Quadratic Gaussian Optimal Control Modification for Flutter Suppression of Adaptive Wing," AIAA Infotech@Aerospace Conference, AIAA 2015-0118, January 2015.

[2]Nguyen, N. and Balakrishnan, S. N.,"Bi-Objective Optimal Control Modification Adaptive Control for Systems with Input Uncertainty," IEEE/CAA Journal of Automatica Sinica, Vol. 1, No. 4, pp. 423-434, October 2014.

[3]Nguyen, N., "Multi-Objective Optimal Control Modification Adaptive Control Method for Systems with Input and Unmatched Uncertainties," AIAA Guidance, Navigation, and Control Conference, AIAA-2014-0454, January 2014.

[4]Nguyen, N., "Bi-Objective Optimal Control Modification Adaptive Control for Systems with Input Uncertainty," AIAA Guidance, Navigation, and Control Conference, AIAA-2012-4615, August 2012.

[5]Nguyen, N. and Urnes, J., "Aeroelastic Modeling of Elastically Shaped Aircraft Concept via Wing Shaping Control for Drag Reduction," AIAA Atmospheric Flight Mechanics Conference, AIAA-2012-4642, August 2012.

[6]Nguyen, N. and Tal, E., "A Multi-Objective Flight Control Approach for Performance Adaptive Aeroelastic Wing," 56th AIAA/ASME/ASCE/AHS/SC Structures, Structural Dynamics, and Materials Conference, AIAA-2015-1843, January 2015.

[7]Nguyen, N., Ting, E., Chaparro, D., Drew, M., and Swei, S., "Multi-Objective Flight Control for Drag Minimization and Load Alleviation of High-Aspect Ratio Flexible Wing Aircraft," Structural Dynamics Conference, January 2017.

[8]Nguyen, N., "Least-Squares Model Reference Adaptive Control with Chebyshev Orthogonal Polynomial Approximation," AIAA Journal of Aerospace Information Systems, Vol. 10, No. 6, pp. 268-286, June 2013.

[9]Nguyen, N., "Optimal Control Modification for Robust Adaptive Control with Large Adaptive Gain," Systems & Control Letters, 61 (2012) pp. 485-494.

[10]Nguyen, N., Krishnakumar, K., and Boskovic, J., "An Optimal Control Modification to Model Reference Adaptive Control for Fast Adaptation," AIAA Guidance, Navigation, and Control Conference, AIAA-2008-7283, August 2008.

[11]Nguyen, N., "Elastically Shaped Future Air Vehicle Concept," NASA Innovation Fund Award 2010 Report, October 2010, Submitted to NASA Innovative Partnerships Program, http://ntrs.nasa.gov/archive/nasa/casi.ntrs.nasa.gov/20110023698.pdf

[12]Nguyen, N., Trinh, K., Reynolds, K., Kless, J., Aftosmis, M., Urnes, J., and Ippolito, C., "Elastically Shaped Wing Optimization and Aircraft Concept for Improved Cruise Efficiency," AIAA Aerospace Sciences Meeting, AIAA-2013-0141, January 2013.

[13]Boeing Report No. 2012X0015, "Development of Variable Camber Continuous Trailing Edge Flap System," October 4, 2012.

[14]Urnes, J., Nguyen, N., Ippolito, C., Totah, J., Trinh, K., and Ting, E., "A Mission Adaptive Variable Camber Flap Control System to Optimize High Lift and Cruise Lift to Drag Ratios of Future N+3 Transport Aircraft," AIAA Aerospace Sciences Meeting, AIAA-2013-0214, January 2013.

[15]Kokotovic, P., Khalil, H., and O'Reilly, J., *Singular Perturbation Methods in Control: Analysis and Design*, Society for Industrial and Applied Mathematics, 1987.